Available online at www.sciencedirect.com
ScienceDirect
Journal of Pharmaceutical and Biomedical Analysis 46 (2008) 617–624
JOURNAL OF PHARMACEUTICAL AND BIOMEDICAL ANALYSIS
www.elsevier.com/locate/jpba

# The hydration/dehydration behavior of aspartame revisited

C. Guguta, H. Meekes, R. de Gelder*

*Institute for Molecules and Materials, Radboud University Nijmegen, Toernooiveld 1, 6525 ED Nijmegen, The Netherlands*

Received 14 August 2007; received in revised form 19 November 2007; accepted 19 November 2007
Available online 3 December 2007

**Abstract**

Aspartame, L-aspartyl-L-phenylalanine methyl ester, has two hydrates (IA and IB), a hemi-hydrate (IIA) and an anhydrate (IIB). The hydration/dehydration behavior of aspartame was investigated using hot-humidity stage X-ray powder diffraction (XRPD) and molecular mechanics modeling in combination with differential scanning calorimetry (DSC) and thermogravimetric analysis (TGA). The results of this study are compared to earlier studies on aspartame as described in literature. It is shown that earlier transition studies were hampered by incomplete conversions and wrong assignment of the forms. The combination of the techniques applied in this study now shows consistent results for aspartame and yields a clear conversion scheme for the hydration/dehydration behavior of the four forms.


*Keywords:* Aspartame; Hydration; Dehydration; Hot-humidity stage X-ray powder diffraction; Molecular mechanics modeling; Thermogravimetric analysis

## 1. Introduction

Pharmaceutical solids have the tendency to crystallize in multiple crystal forms and the significance of this phenomenon, polymorphism, has been demonstrated through the years [1]. Like polymorphs, the hydrates of an active pharmaceutical ingredient or of an excipient may differ in key properties such as solubility, dissolution rate, stability, and particle habit. Unlike polymorphs, hydrates represent different chemical entities as defined by the stoichiometry of water with respect to the active compound. Depending upon the nature of the hydrate, the water content may change over time with ambient humidity, temperature, or other processing conditions. A well-known example in industry is the "caking" phenomenon attributed to (re)crystallization of a form during storage, often induced by humidity. As a result, the need to identify and evaluate the hydration states available to an active pharmaceutical ingredient or an excipient is as great as the need to assess polymorphism.

Aspartame, L-aspartyl-L-phenylalanine methyl ester, is a dipeptide sweetener increasingly used in pharmaceuticals, food and beverages. The molecular structure of aspartame (APM) is presented in Fig. 1.

In 1983, Chauvet et al. reported on the kinetics of desolvation and decomposition of aspartame [2]. Two years later, in 1985, the crystal structure of aspartame hemi-hydrate form IIA was described by Hatada et al. [3]. Aspartame hemi-hydrate (IIA) crystallizes in the tetragonal system with space group $P4_1$ and cell parameters: $a = 17.685(5)$ Å, $c = 4.919(2)$ Å, $V/Z = 384.615$ Å$^3$. Kishimoto and Naruse reported in 1988 on the morphology and process development of aspartame, demonstrating that the large-scale crystallization process is technically and economically possible [4]. Almost 9 years later, in 1997, Leung and Grant presented stability studies of aspartame and aspartylphenylalanine, showing that such model dipeptides undergo solid-state intra-molecular aminolysis by the elimination of methanol [5]. In the case of aspartame, this process leads to the cyclic compound diketopiperazine (DKP) as the exclusive solid product.

In 1998, Leung et al. described the existence of two polymorphs of aspartame hemi-hydrate, pointing actually to hydrate form IB and hemi-hydrate form IIA [6]. In the same year, the authors described the hydration and dehydration process for the hemi-hydrate form IIA and the existence of four forms for aspartame [7]. They also provided a conversion scheme for the four (hydrate) forms of aspartame, based on differential scanning calorimetry (DSC), hot-stage X-ray powder diffraction (XRPD)

* Corresponding author at: Molecular Materials, Institute for Molecules and Materials, Radboud University Nijmegen, Toernooiveld 1, 6525 ED Nijmegen, The Netherlands. Tel.: +31 24 3652842; fax: +31 24 3553450.
*E-mail address:* R.deGelder@science.ru.nl (R. de Gelder).
*URL:* http://www.crystallography.nl (R. de Gelder).

0731-7085/$ – see front matter © 2007 Elsevier B.V. All rights reserved.
doi:10.1016/j.jpba.2007.11.044

and humidity experiments. Meguro et al. reported in 2000 on the crystal structure of the "low-humidity" form IB determined from single-crystal X-ray diffraction data [8]. The hydrate form IB crystallizes in the monoclinic system with space group $P2_1$ and cell parameters: $a = 22.96(2)$ Å, $b = 4.964(5)$ Å, $c = 23.50(2)$ Å, $\beta = 123.2(1)^\circ$, $V/Z = 373.528$ Å$^3$. In the same year, Rastogi et al. presented a study of the decomposition behavior of the hemi-hydrate form IIA using real-time hot-stage XRPD [9]. The authors also discussed the decomposition of aspartame, concluding that the amount of the reaction product increases with increasing temperature. In 2004, Cuppen et al. described the needle-like morphology of aspartame crystals by means of Monte Carlo simulations [10].

One year later, Cuppen et al. reported on the crystal structure of the hydrate form IA and the morphology prediction for this form [11]. The water richest hydrate form IA crystallizes in the monoclinic system with space group $P2_1$ and cell parameters: $a = 25.450(2)$ Å, $b = 4.8795(9)$ Å, $c = 23.749(2)$ Å, $\beta = 116.468(8)^\circ$, $V/Z = 440.02$ Å$^3$.

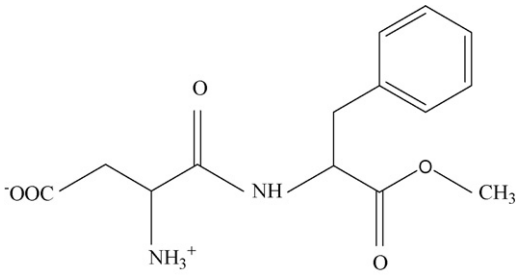


Fig. 1. The molecular structure of aspartame.

The crystal structure of the anhydrate form of aspartame (IIB) was recently described by Guguta et al. [12]. The anhydrate form IIB crystallizes in the monoclinic system with space group $P2_1$ and cell parameters: $a = 19.4078(10)$ Å, $b = 4.9605(2)$ Å, $c = 15.6547(9)$ Å, $\beta = 94.876(2)^\circ$, $V/Z = 375.412$ Å$^3$. An overview of the crystal structures of the four forms of aspartame is presented in Fig. 2 [13].

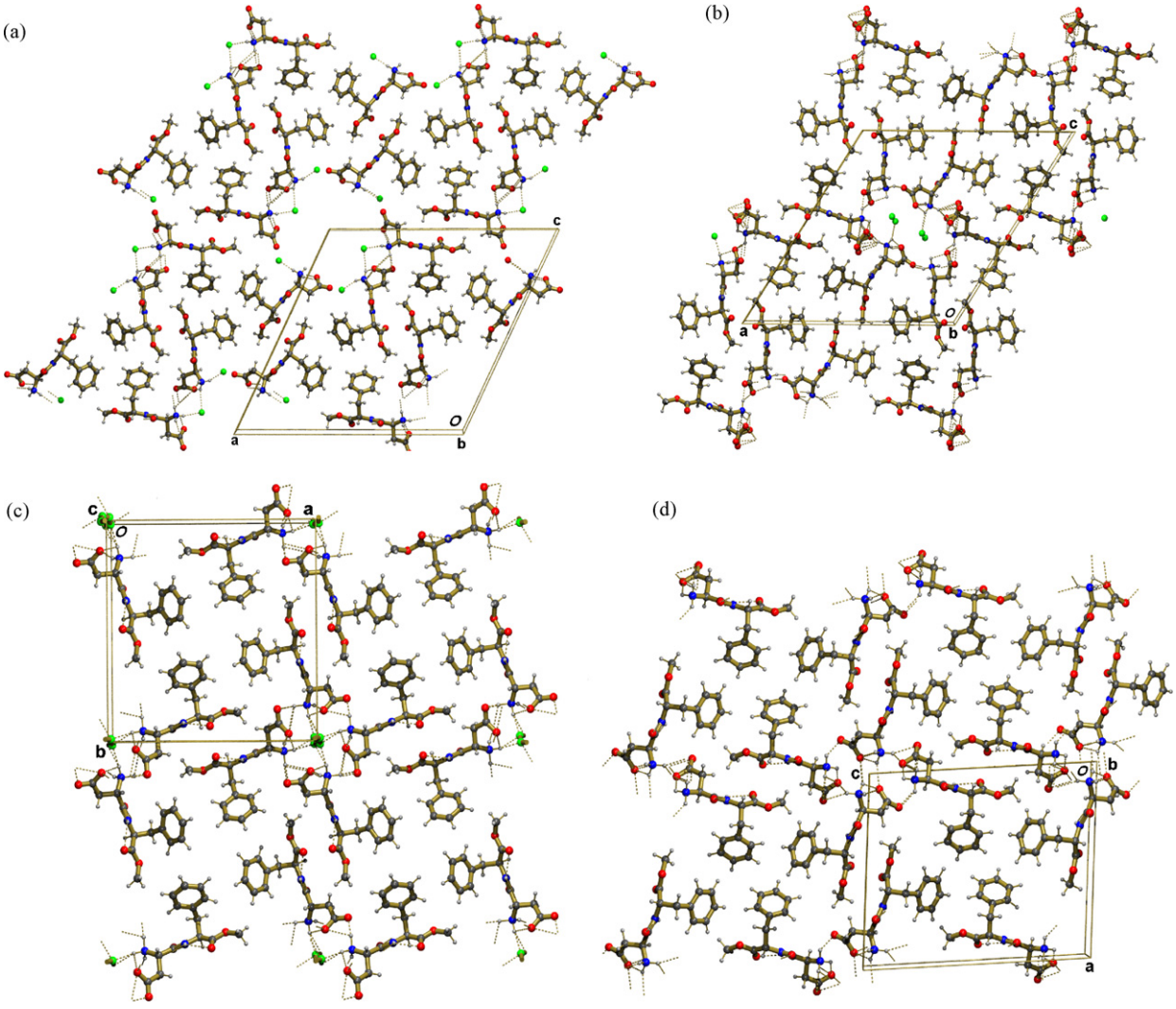


Fig. 2. Projections along the short axis of the unit cell for: (a) hydrate form IA (CSD refcode EFIFOO01); (b) hydrate form IB (CSD refcode ODOBAK); (c) hemi-hydrate form IIA (CSD refcode DAWGOX); (d) anhydrate IIB (CSD refcode KETXIR); water molecules are indicated in green.

A high degree of similarity between the structures of hydrate form IA and form IB can be observed. In the case of form IA, the hydrophilic channel is made up of both water and aspartame molecules. Inside the channels, the remaining water molecules are disordered as they are loosely bound to the skeleton [11]. Hydrate form IB contains hydrophilic channels made up of only aspartame molecules and the water molecules can be found only inside these channels. The hydrophobic sides of aspartame, the phenyl rings, are grouped in triples for the hydrate forms IA and IB. During dehydration of the water richest form IA (14% hydration water corresponding to 2.6 molecules $H_2O$/molecule aspartame), the principal packing does not change, but instead, the hydrate channels become smaller. The hydrate form IB contains a smaller amount of hydration water (3.9% hydration water corresponding to 0.67 molecule $H_2O$/molecule aspartame) and accordingly the ratio *V/Z* (cell volume/number of aspartame molecules in the cell) is significantly smaller for the IB form (373.528 $Å^3$) than for the IA form (440.02 $Å^3$).

For the case of the hemi-hydrate and anhydrate forms, a different relation was noticed between the crystal structures [12]. Both the hydrophobic and hydrophilic sides of aspartame are grouped in quadruples in these forms. Hemi-hydrate form IIA has hydrophilic channels made up of only aspartame molecules and the water molecules can be found only inside these channels. Apparently, by dehydrating the hemi-hydrate (3% hydration water corresponding to 0.5 molecule $H_2O$/molecule aspartame), the water disappears from the channels, the structure collapses slightly and the tetragonal symmetry breaks down to give a monoclinic one.

Altogether, aspartame is a well-studied and interesting system with respect to its hydration/dehydration behavior. However, combining all the information existent in the literature about conditions and possibilities for conversions and trying to match the recently available structural information of all forms IA, IB, IIA, and IIB with the forms identified and described in the literature, leads to confusing and contradictory results. The various assignments of pure forms seem to be hampered by incomplete conversions leading to different conditions for transitions.

Therefore, this study is aimed to provide a detailed insight into the hydration and dehydration behavior of aspartame, down to the molecular level, using hot-humidity stage X-ray powder diffraction and molecular mechanics modeling in combination with differential scanning calorimetry and thermogravimetric analysis.

## 2. Experimental

### 2.1. Preparation of the four forms of aspartame

Hydrate form IA was prepared from a saturated solution of commercially available aspartame in water (1.16 g APM: 100 mL $H_2O$) at room temperature. After a few hours small needle shaped crystals already formed. To avoid the dehydration of the sample before the measurements, the adhering water solution was not removed.

Hydrate form IB was obtained from a saturated solution of commercially available aspartame in water, heated to 50 °C (2.6 g APM: 100 mL $H_2O$) and allowed to cool to room temperature. After 1 week, the solvent solution was evaporated completely and a layer of needle shaped crystals was formed.

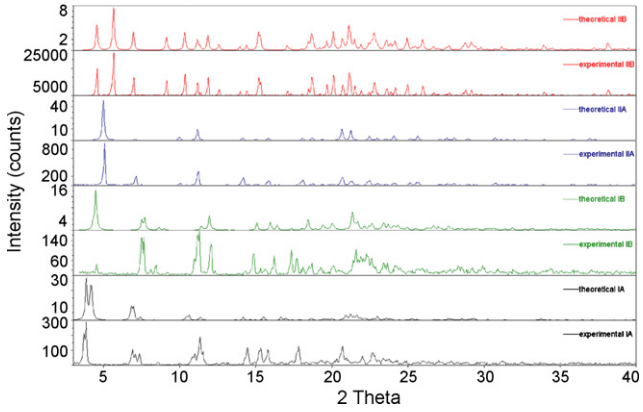


Fig. 3. The experimental X-ray powder diffraction patterns of: hydrate form IA; hydrate form IB; hemi-hydrate form IIA; anhydrate form IIB together with the simulated patterns of the forms.

Hemi-hydrate form IIA was prepared at room temperature from a saturated solution of commercially available aspartame in water, by mixing it with an equal volume of a solution made of 20% acetone, 20% ethanol, 10% dimethyl sulfoxide and 50% water [7]. After 4 days, the solvent solution was evaporated completely and a layer of needle shaped crystals was formed.

The anhydrate form IIB can be obtained by dehydrating the hemi-hydrate form IIA at 90 °C. Exposure to air of the anhydrate form IIB leads immediately to conversion to the hemi-hydrate form IIA and therefore IIB form was stored in a glove box under nitrogen atmosphere.

The purity of all four forms of aspartame was checked using X-ray powder diffraction (Fig. 3).

### 2.2. Analytical methods

#### 2.2.1. Hot-humidity stage X-ray powder diffraction (XRPD)

X-ray powder diffraction was performed on the investigated samples using a Bruker D8 AXS Advance X-ray Diffractometer with hot-humidity stage and VÅNTEC-1 detector. The diffractometer was equipped with a Johansson type monochromator. The detector was set at an effective angular region of 2°. The data were collected in reflection geometry using monochromatic Cu $K\alpha_1$ radiation. The most important instrumental and data collection parameters are presented in Table 1.

Table 1
Instrumental and data collection parameters

| Typical measuring conditions | |
|---|---|
| Range (° 2$\theta$) | 2–40 |
| Step size (° 2$\theta$) | 0.05 |
| Step time (s) | 1 |
| Relative humidity (%RH) | 0–80 |
| Temperature range (°C) | 25–125 |
| Heating rate (°C/min) | 1 |
| Carrier gas | Nitrogen |

#### 2.2.2. Differential scanning calorimetry (DSC)

Differential scanning calorimetry curves were obtained using a Mettler Toledo 822 DSC with a TSO 801RO Sample Robot. The instrument was temperature calibrated using indium standards. The samples were scanned at 0.5 or 1 °C/min from 20 to 250 °C under nitrogen purge at 40 mL/min in pierced aluminum pans.

#### 2.2.3. Thermogravimetric analysis (TGA)

Thermogravimetric analysis curves were generated using a TA Instruments Q500 TGA. The instrument was temperature calibrated using indium, tin and zinc standards. A weight calibration was performed using standard weights under nitrogen purge. The samples were scanned at 1 °C/min from 20 to 250 °C under nitrogen purge at 40 mL/min in pierced aluminum pans.

### 2.3. Molecular mechanics modeling

For molecular mechanics modeling, Cerius[2] with the Dreiding force field was used. The electrostatic and van der Waals interactions were calculated using Ewald summation and Gasteiger point charges [14].

## 3. Results and discussion

### 3.1. Hot-humidity stage X-ray powder diffraction

The complete conversions recorded with hot-humidity stage X-ray powder diffraction for the hydrate forms IA and IB and hemi-hydrate form IIA are presented in Fig. 4.

Hot-humidity stage X-ray powder diffraction was first performed on samples of the water richest form IA. During the hydration of form IA at 40 °C and 80%RH for 12 h, no other forms with a higher amount of hydration water were observed. After dehydrating form IA in a temperature range between 45 and 85 °C at 0%RH, hydrate IB is formed. In order to study the reverse process, *i.e.* the conversion of the hydrate IB to form IA, form IB was hydrated at 40 °C and 80%RH. After 30 min at 40 °C and 80%RH a complete conversion to form IA was observed (Fig. 4a).

By dehydrating form IB in a temperature interval of 25–125 °C at 0%RH, a complete conversion to the anhydrate form IIB was observed (Fig. 4b). No intermediate conversion to the hemi-hydrate form IIA was observed.

To study the dehydration of the hemi-hydrate form IIA, the crystallized form IIA was heated in a temperature range between 40 and 85 °C at 0%RH. A complete conversion to the anhydrate form IIB was already observed at 40 °C. Leaving the anhydrate form IIB at 40 °C and 80%RH for 140 min resulted in the reverse formation of form IIA (Fig. 4c). Continued exposure of the hemi-hydrate form IIA to 80%RH and 40 °C, did not lead to any further conversion.

If we compare our results with the conversion scheme reported by Leung et al. in 1997, we find significant differences. The X-ray powder diffraction patterns of the converted forms described by Leung et al. do not correspond to pure forms but to mixtures, as can be concluded from the crystal structures of the four forms now available. Leung et al. state that reversible conversions take place between aspartame "di-hemi-hydrate" and "hemi-hydrate form II". The dehydration of the "hemi-hydrate form II" leads to the anhydrate form. The aspartame "hemi-hydrate form I" can be hydrated to the "di-hemi-hydrate". During the dehydration of the "hemi-hydrate form I", the anhydrate is formed. Leung et al. also state that dehydration of the "hemi-hydrate form II" leads to the "hemi-hydrate form I". We can now reinterpret the conversion scheme of Leung et al. In terms of forms IA, IB, IIA and IIB, the scheme shows that their hemi-hydrate form II is in fact hydrate form IB and their "di-hemi-hydrate" is in fact the water richest hydrate form IA which contains considerably more water than the presumed monohydrate. Their hemi-hydrate form I corresponds to our hemi-hydrate form IIA and their anhydrate to our anhydrate form IIB. The main discrepancy between the conversion scheme of Leung et al. and ours is that we do not find a conversion from form IIA to form IA and we also do not find a conversion from form IB to form IIA. In addition, Leung et al. attempted to investigate the susceptibility of aspartame "hemi-hydrate" to polymorphic transitions by ball-milling at elevated temperatures and compression. Pointing towards a "mechanical activation" of the solid fractions as a final result, the decreased crystallinity of the obtained forms unfortunately hampered the solid-state characterization of the investigated forms. On the other hand, we found that milled material when used as such for conversion experiments often shows incomplete conversions. Our study shows that for all conversions pure forms, in principal, can be obtained. Therefore, we attribute this discrepancy between our results and those of Leung et al. to our use of crystalline material that was not ground before experiments and to the extreme hygroscopicity of the anhydrate form.

### 3.2. Thermal analysis

Thermal analysis can provide information on the nature of the hydrate and proof of the hydration level. Differential scanning calorimetry and thermogravimetric analysis were applied to both hydrates (IA and IB) and hemi-hydrate (IIA). As expected, each of the forms yielded unique DSC and TGA signatures.

#### 3.2.1. Differential scanning calorimetry

Differential scanning calorimetry curves of hydrates IA, IB and hemi-hydrate IIA at different heating rates are shown in Fig. 5.

In order to avoid the dehydration of the sample, the adhering water from the IA crystals was not removed before the measurement was carried out. Otherwise, the sample would already have partly converted into the hydrate form IB. The DSC measurement of hydrate form IA, applying a heating rate of 0.5 °C/min, exhibits two endothermic events between 20 and 100 °C due to solvent loss, corresponding to the formation of the hydrate form IB and, respectively, to the formation of the anhydrate form IIB (also suggested by the results obtained with hot-humidity stage X-ray powder diffraction). The first endothermic effect is remarkably large due to the removal of adsorbed water molecules and the water molecules incorporated in the crystal structure on

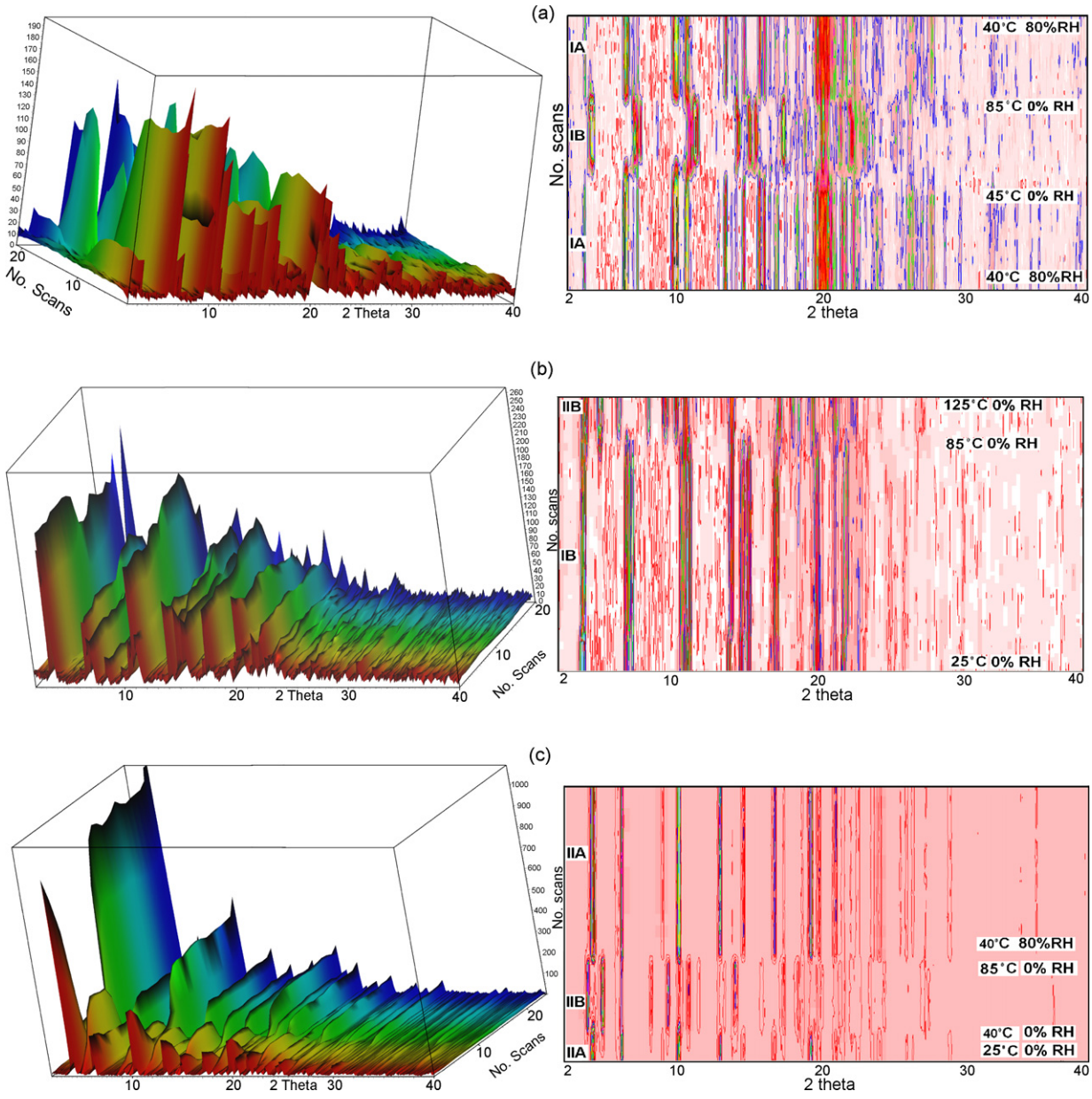


Fig. 4. 3D pictures (left) and top views (right) of the hot-humidity stage X-ray powder diffraction experiments: (a) the conversion of hydrate form IA to form IB and back to hydrate form IA; (b) the conversion of hydrate form IB to anhydrate form IIB; (c) the conversion of hemi-hydrate form IIA to anhydrate form IIB and back to hemi-hydrate form IIA.

one hand, and to the degradation of aspartame on the other hand (Fig. 5a). It is known that in aqueous solution, aspartame hydrolyses to form aspartylphenylalanine and phenylalanine methyl ester, competing with diketopiperazine formation [5]. Using a higher heating rate (1 °C/min), the presence of the second endothermic event becomes uncertain but the hot-humidity stage X-ray powder diffraction experiments at the same heating rate supports the presence of this event.

The DSC measurement of hydrate form IB (Fig. 5b) shows an endothermic event due to solvent loss at temperatures between 80 and 120 °C confirming once again the results obtained with hot-humidity stage X-ray powder diffraction.

DSC analysis recorded for the sample of hemi-hydrate form IIA exhibits an endothermic event at temperatures between 20 and 50 °C indicating the loss of solvent and the formation of the anhydrate IIB (Fig. 5c).

Both hydrates and the hemi-hydrate exhibit two endothermic events in the region from 160 to 250 °C for a heating rate of 1 °C/min. The endothermic event recorded around 160 °C, corresponding to the decomposition of aspartame, is significantly smaller when starting with form IA compared to the results when starting with form IB or IIA, due to prior decomposition of the sample. The endothermic event is attributed to a cyclization reaction, which involves an intra-molecular aminolysis with release of methanol to form the cyclic compound diketopiperazine, which is in a good agreement with the findings of Leung and Grant [5]. The second endothermic event observed at 230 °C indicates the melting of the DKP. The DSC measurement

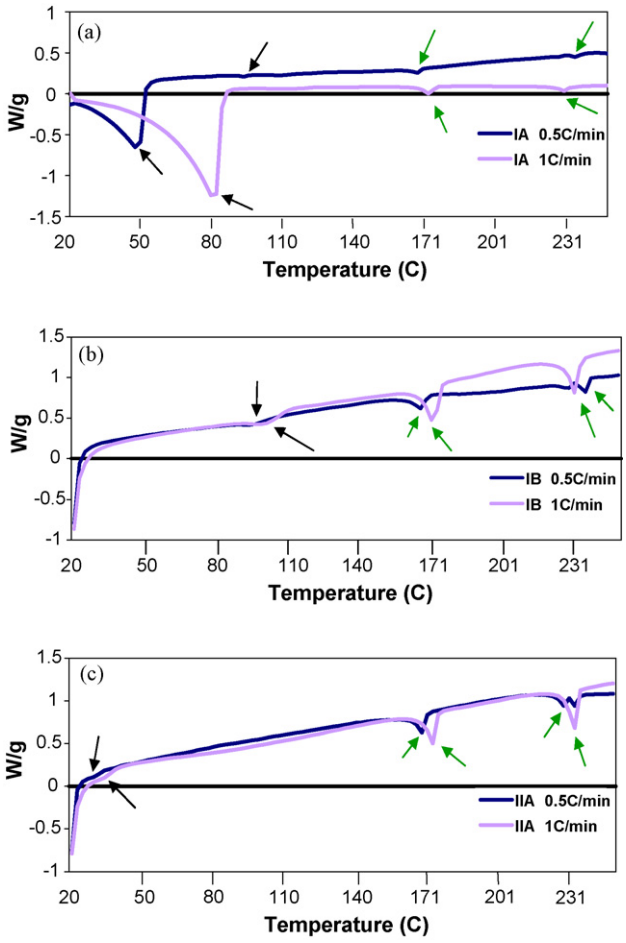


Fig. 5. DSC curves recorded for: (a) hydrate IA; (b) hydrate IB; (c) hemi-hydrate IIA (the endothermic events are pointed out with arrows).

recorded with 0.5 °C/min for the hemi-hydrate form IIA exhibits an endothermic event at 230 °C indicating the decomposition of DKP and another endothermic effect at 235 °C, indicating the melting of the decomposition compound. The shifts recorded for all the investigated forms with 1 °C/min in comparison with the ones observed at 0.5 °C/min are attributed to the higher heating rate.

### 3.2.2. Thermogravimetric analysis

TGA curves and their derivatives of the investigated hydrates (IA and IB) and hemi-hydrate (IIA) are presented in Fig. 6.

Hydrate IA exhibited a remarkably high weight loss of 82.36% in a temperature range from 20 to 120 °C. In order to avoid the dehydration of the sample into the hydrate form IB, the adhering water solution from the IA crystals was not removed. Taking also into account that aspartame readily degrades in an aqueous solution, it is impossible to distinguish between the loss of weight caused by the removal of adsorbed water molecules, the loss due to the removal of water molecules incorporated in the crystal structure and the one corresponding to the degradation process (Fig. 6a). It seems that like in aqueous solution, the presence of adhered water allows the hydrolysis of aspartame to form aspartylphenylalanine and phenylalanine methyl ester, to compete with diketopiperazine formation [5]. Determination of an exact temperature range corresponding to the formation of hydrate IB and anhydrate IIB from hydrate IA is impossible using TGA alone.

For hydrate form IB, the TGA curve shows a weight loss of 3.469% (0.59 molecule $H_2O$/molecule aspartame) in a temperature range from 20 to 130 °C, which can be associated with the formation of the anhydrate IIB (Fig. 6b). In this case, the data obtained from TGA are in accordance with the data obtained from hot-humidity stage X-ray powder diffraction and DSC.

In a temperature range from 20 to 130 °C, the TGA curve of the hemi-hydrate IIA exhibits a two-step weight loss corresponding to 0.38 molecule $H_2O$/molecule aspartame in total (Fig. 6c). This might be an indication that the hemi-hydrate IIA can convert upon heating to another form and finally to the anhydrate form. This could, however, not be confirmed by DSC or hot-humidity stage X-ray powder diffraction.

All investigated forms of aspartame decomposed at 170 °C and the decomposition product DKP melted at temperatures between 230 and 250 °C. As found in the DSC measurements, the weight loss recorded at 170 °C, corresponding to the decomposition of aspartame, is significantly smaller when starting with form IA as compared to the results when starting with form IB or IIA, due to prior decomposition of the sample. The decomposition of aspartame results in the release of methanol with a theoretical weight loss of 10.55% close to the observed weight loss of 10.24% for the hydrate form IB and, respectively, 10.49% for the hemi-hydrate form IIA. This shows that almost all aspartame is decomposed.

### 3.3. Molecular mechanics modeling

To shed more light on the role of the water molecules in form IA and to mimic the conversion of form IA to IB by dehydration, a number of energy minimization experiments were carried out in analogy with the experiments successfully performed earlier for the dehydration of form IIA [12]. The most obvious strategy to mimic dehydration of the IA form is the removal of some water molecules from the channels in $P2_1$ and the minimization of the resulting structure. The inconvenience in this case is that the water molecules inside the channels are disordered and loosely bound to the skeleton, whereas the water molecules making up the channels are relatively strongly bonded to the aspartame architecture. The second problem is that not all water molecules inside the channels were well determined by single-crystal X-ray diffraction. Nevertheless, partial removal of water molecules, by removing two of the water molecules making up the channel and placing the other two water molecules at an arbitrary position inside the channel followed by minimization of the energy, leads to a packing similar to the hydrate form IB minimized (Fig. 7a). Removing all water molecules existent in hydrate form IA and minimizing the structure again, also leads to such a structure (Fig. 7b). In Table 2, the unit cell parameters of the structures of hydrate IB, minimized hydrate IB, hydrate IA minimized in $P2_1$ after partial removal of the water molecules and hydrate IA minimized in $P2_1$ after removal of all water molecules are presented.

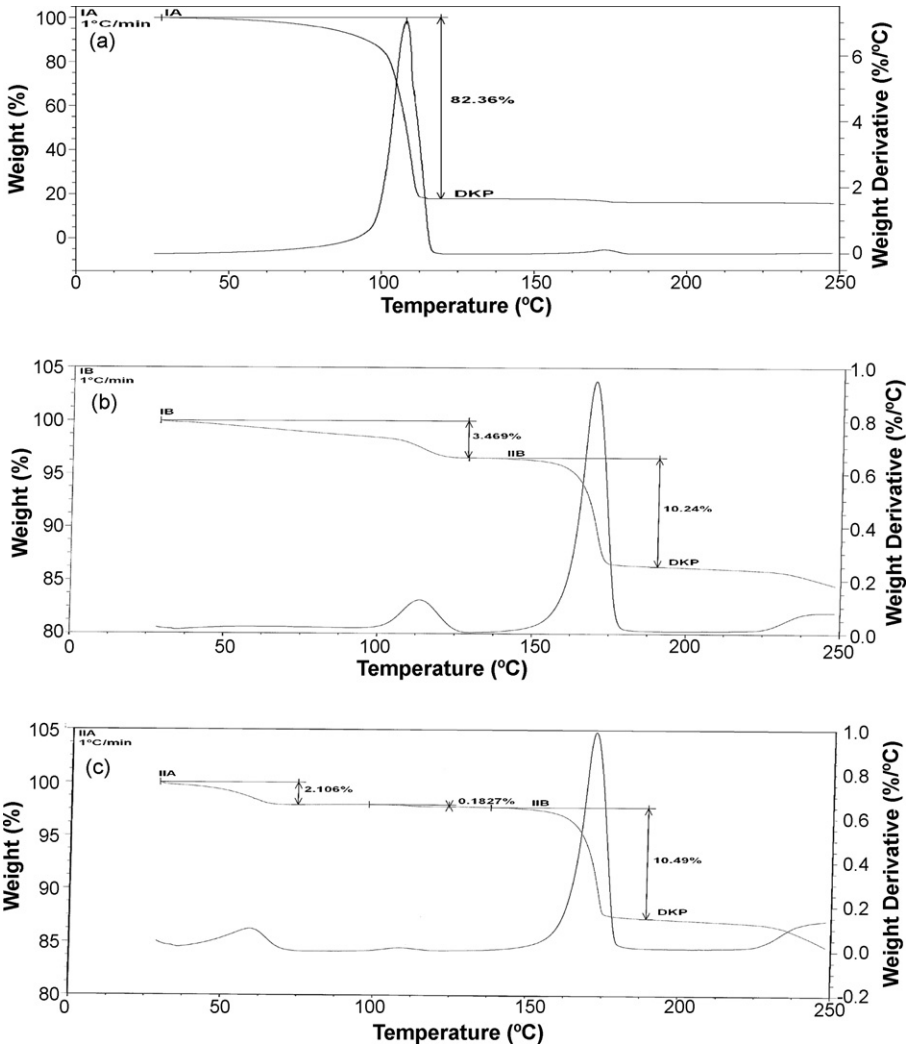


Fig. 6. TGA and derivative curves (1 °C/min) for: (a) hydrate form IA; (b) hydrate form IB; (c) hemi-hydrate form IIA.

Repeating the minimization experiments with partial removal of water molecules but now reducing the space group symmetry of the structure to P1, which opens the possibility for symmetry breaking, yields a result that is almost similar to the one obtained before. Minimizing this structure in P1 imposes no specific symmetry on the system and might result, in principle, in a structure with other or lower symmetry than P21. Apparently, in the case of aspartame forms IA and IB the water molecules do not play

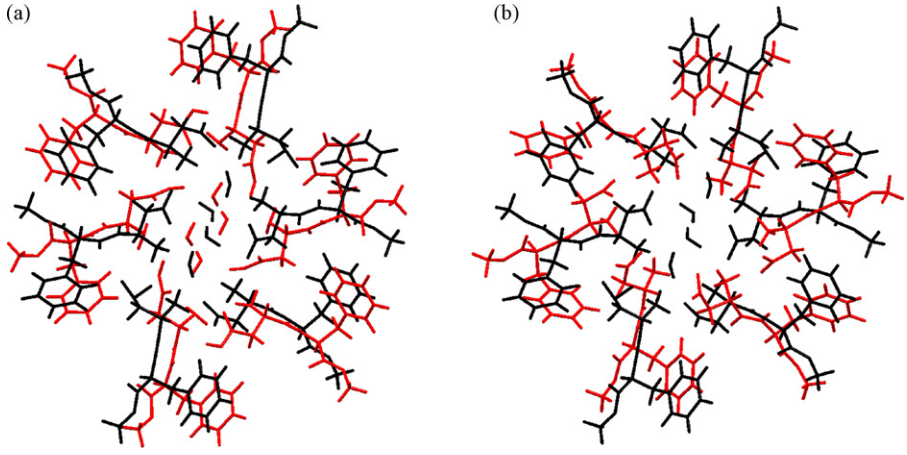


Fig. 7. Comparison between the crystal structures of: (a) the minimized hydrate IB (black) and hydrate IA minimized in $P2_1$ after partial removal of two water molecules (red); (b) the minimized hydrate IB (black) and hydrate IA minimized in $P2_1$ after removing all water molecules (red). (For interpretation of the references to color in this figure legend, the reader is referred to the web version of the article.)

Table 2
Comparison between the hydrate IB and the minimized IA structures

| Unit cell parameters | IB (CSD refcode ODOBAK) | Minimized IB | Minimized IA after partial removal of water molecules | Minimized IA after removal of all water molecules |
|---|---|---|---|---|
| $a$ (Å) | 22.96(2) | 23.06 | 23.03 | 23.35 |
| $b$ (Å) | 4.964(5) | 5.06 | 4.95 | 5.29 |
| $c$ (Å) | 23.50(2) | 23.78 | 23.92 | 23.43 |
| $\beta$ (°) | 123.20(1) | 118.88 | 117.06 | 123.80 |
| $V$ (Å$^3$) | 2241.17 | 2430.60 | 2429.22 | 2408.07 |

an important role in maintaining the monoclinic symmetry. This might have been expected for the water molecules inside the channels, but surprisingly even holds for the water molecules that make up the channels of form IA.

## 4. Conclusions

The hydration/dehydration behavior of aspartame was investigated using hot-humidity stage X-ray powder diffraction and molecular mechanics modeling in combination with differential scanning calorimetry and thermogravimetric analysis.

The combination of the applied techniques shows consistent results for aspartame and yield a clear conversion scheme for the four forms. They also indicate that application of hot-humidity stage X-ray powder diffraction gives more detailed information.

Hot-humidity stage X-ray powder diffraction showed reversible and complete conversions between the two hydrates IA and IB, and between the hemi-hydrate IIA and anhydrate IIB. Using the same technique, the irreversible conversion upon heating between hydrate form IB and anhydrate IIB was also observed. The conversions can be summarized in the following scheme:

$$\mathrm{IA} \underset{40^\circ\mathrm{C}+80\%\mathrm{RH}}{\overset{25-85^\circ\mathrm{C}+0\%\mathrm{RH}}{\rightleftarrows}} \mathrm{IB} \xrightarrow{85-125^\circ\mathrm{C}+0\%\mathrm{RH}} \mathrm{IIB} \underset{40-85^\circ\mathrm{C}+0\%\mathrm{RH}}{\overset{40^\circ\mathrm{C}+80\%\mathrm{RH}}{\rightleftarrows}} \mathrm{IIA}$$

Hot-humidity stage X-ray powder diffraction offers a convenient way to follow both hydration and dehydration with respect to time, showing in particular the completeness of the conversions.

Comparison of the two hydrates IA and IB revealed a remarkable similarity between the crystal structures. Molecular modeling experiments for the conversion of form IA to form IB suggest that the water molecules do not play an important role in maintaining the overall structure and the monoclinic symmetry of form IA. On removal of the water molecules in various ways and to various extents the packing of the aspartame molecules around the channels attains a similar motif. The major structural change is a shrinkage of the channel diameter.

Comparing our experimental results with the structural information of the four forms of aspartame shows that a number of forms described in literature are wrongly assigned or correspond to mixtures. The systematic study on aspartame as presented in this paper may be of importance for a further understanding of the formation of hydrates and shows that the availability of crystal structures together with analytical data provides a detailed insight into the hydration/dehydration behavior of compounds.

## Acknowledgments

This research was supported by the Technology Foundation STW, applied science division of NWO and the technology programme of the Ministry of Economic Affairs. I. Eeuwijk is also acknowledged for performing TGA measurements.

## References

[1] Y. Cui, Int. J. Pharm. 339 (2007) 3–18.
[2] A. Chauvet, H. Saint-Julien, G. De Maury, J. Masse, Thermochim. Acta 71 (1983) 79–91.
[3] M. Hatada, J. Jancarik, B. Graves, S. Kim, J. Am. Chem. Soc. 107 (1985) 4279–4282.
[4] S. Kishimoto, M. Naruse, J. Chem. Technol. Biotechnol. 43 (1988) 71–82.
[5] S.S. Leung, D.J.W. Grant, J. Pharm. Sci. 86 (1997) 64–71.
[6] S.S. Leung, B.E. Padden, E.J. Munson, D.J.W. Grant, J. Pharm. Sci. 87 (1998) 501–507.
[7] S.S. Leung, B.E. Padden, E.J. Munson, D.J.W. Grant, J. Pharm. Sci. 87 (1998) 508–513.
[8] T. Meguro, T. Kashiwagi, Y. Satow, J. Pept. Res. 56 (2000) 97–104.
[9] S. Rastogi, M. Zakrewski, R. Suryanarayanan, Pharm. Res. 3 (2001) 267–273.
[10] H.M. Cuppen, A.R.T. van Eerd, H. Meekes, Cryst. Growth Des. 5 (2004) 989–997.
[11] H.M. Cuppen, G. Beurkens, S. Kozuka, K. Tsukamoto, J.M.M. Smits, R. de Gelder, R.F.P. Grimbergen, H. Meekes, Cryst. Growth Des. 5 (2005) 917–923.
[12] C. Guguta, H. Meekes, R. de Gelder, Cryst. Growth Des. 4 (2006) 989–997.
[13] A.L. Spek, Acta Cryst. A46 (1990) C34.
[14] Cerius2 2002, User Guide, Accelrys Inc. San Diego, USA.